TELKOMNIKA, Vol. 11, No. 6, June 2013, pp. 2912 ~ 2925
e-ISSN: 2087-278X

A Comparative Control Method for Induction Motor and High Performance Z-source Inverter

Cong-Thanh Pham*, An Wen Shen[2]
Department of Control Science and Engineering, HuaZhong University of Science and Technology, 1037 LuoYu Road, WuHan, HuBei, China, telp:008613986059057
Corresponding author, e-mail: phamcongthanh1978@gmail.com, sawyi@mail.hust.edu.cn

Abstract

Design studies of the most suitable controller for the speed of induction motor (SIM) and peak DC-link voltage (PDV) of high performance z-source inverter (HP-ZSI) greatly affects performance of hybrid electric vehicles. This paper is to give comprehensive analyses *comparison and evaluations of the different control techniques as PI controller, self-tuning fuzzy PI controller (SFP) and genetic algorithms optimal tuning gains of the PI controller for controlling the SIM based on criteria of the integral of the absolute value of speed error (IAE). With control PDV, this paper also presents comparisons of the different techniques as PI controller, fuzzy logic controller, SFP based on observation of its response and total harmonic distortion of current. All methods are applied to the closed loop of the SIM which relies on direct torque control combined with modified space vector modulation and closed loop of PDV in HP-ZSI. These methods are verified by Matlab software.*

Keywords*: buck-boost, DTC-SVM, SIM, HP-ZSI.*

1. Introduction

The z-source inverters (ZSI) is a power electronic converter with many advantages such as buck-boost characteristics, lower cost, and especially high efficiency compared to traditional DC-DC converter [1, 2]. In addition, ZSI can be overcome drawbacks in the conventional voltage source inverter (VSI) such as the maximum output voltage can exceed the DC bus voltage, the two switches of any phase leg can be gated at the same time which does not affect the short circuit situation and destroy the inverter [3]. As a more sophisticated design of ZSI, the HP-ZSI copes with DC-link voltage (DCV) drops for a wide range of load even using a small inductor while design guarantee is a simple. Thus, HP-ZSI is more suitable for hybrid electric vehicles (HEV) applications [4, 5].

In HEV drive systems, the control requirements are very high and stringent as well as fast torque response, low torque ripple at steady state, high accuracy, wide speed range, and high torque at low speed. It is really challenging to meet all of these requirements by using traditional control methods of induction motor (IM) such as: voltage/hezt, field oriented control and traditional direct torque control (DTC), but the traditional DTC combined with space vector modulation (DTC-SVM) scheme can succeed in [6-8]. In addition, DTC combined with modified space vector modulation (MSVM) which is called DTC-MSVM. Among them, MSVM base on SVM which the shoot-through state (STS) is used to insert within the switching pattern of SVM. The STS is applied to control DCV of the HP-ZSI [6, 9, 10].

The DCV of HP-ZSI is in square waveform, the relationship between the PDV $(\hat{V}_i)$ and the capacitor voltages are the nonlinear [3, 11]. Consequently, the average value of the DCV (V_i) be controlled by controlling the PDV value. In recent years, some studies have proposed as PI controller and neural network controller which are used to control PDV of the HP-ZSI [10-13]. However, these control methods contain some inherent drawbacks such as slowness in adapting plant parameters, high total harmonic distortion of current, increase the voltage stress across the switching and transient response of PDV are not good while the DC-input voltage (DIV) suddenly changes [5]. Therefore, studies design of the most suitable controller for PDV is very important in the HP-ZSI system.

Received February 21, 2013; Revised March 14, 2013; Accepted April 7, 2013

In nonlinear systems, the operating system parameters are always continuous variation and uncertainties such as parameters of the induction motor, external load disturbance, DIV. Fixed gains of conventional PI controller is not suitable with the required high performance of drive systems [14-17]. Hence, the intelligent control techniques such as fuzzy logic controller (FLC), SFP, genetic algorithms optimal tuning gains of the PI controller (GAs-PI) will promise for this system.

FLC is often used to cope with continuous variation of parameters of nonlinear systems and do not rely on any mathematical models of drive systems which it is still robust control and adapt to the parameter uncertainties of systems based on human knowledge [21]. Thus, many studies have proposed FLC for controlling PDV in HP-ZSI [22]. Especially, FLC is also used to adjust on-line the gains of the PI controller which is called SFP for controlling the PDV [6] and controlling the SIM [6, 25, 26] respectively. However, these controllers have been separately studied in some papers that they did not have a comparison between those controllers with each other to select the most suitable controller for the PDV and SIM.

GAs has been widely used in control industrial applications [17]. GAs is a stochastic global optimization search technique based on the principles of natural selection and genetics [27, 29]. Also, this algorithm has been applied successfully to solve complex optimization problems which it does not need the derivative of the fitness function [27]. The GAs strategy in nonlinear control systems is to determine the parameters of controllers base on the minimization of a fitness function. GAs is proposed to optimize the FLC to increase accuracy, fast convergence and maintain the stability of complex nonlinear systems [27]. In addition, this method was also applied to determine the gains of the conventional PI controller in applications AC drive [17, 29]. However, in order to tune gains of the PI controller on-line, the rate of the microcontroller and the convergence rate of GAs must be required very high.

Despite many studies proposed new controllers are based on adaptive intelligent control technique to cope with continuous variation and uncertainties of parameters in the SIM and PDV of the DTC-MSVM scheme. However, these control techniques have been separately studied in some papers that they did not show a comparison between those control techniques with each other. The aim of this paper is to give a comprehensive analysis comparison and evaluations of the different control strategies such as PI controller, SFP and GAs-PI for controlling the SIM which based on performance criteria as IAE. With control of the PDV, this paper also presents a comparison of the different control techniques such as PI controller, SFP, FLC which based on observation of its response and total harmonic distortion of current. All methods are applied to a closed loop of the SIM and PDV which relies on DTC-MSVM scheme. These methods are verified in simulation implementation using Matlab software.

2. Analysis Induction Motor Model, DTC-MSVM Scheme and HP-ZSI

2.1. Analysis Induction Motor Model

The corresponding stationary frame equations [31] can be derived easily as follows:

Stator Voltage:

$$v_{dqs} = R_s i_{dqs} + \frac{d\varphi_{dqs}}{dt} \tag{1}$$

Rotor voltage:

$$0 = R_r i_{dqr} + \frac{d\varphi_{dqr}}{dt} \pm \omega_r \varphi_{dqr} \tag{2}$$

Stator flux:

$$\varphi_{dqs} = L_{ls} i_{dqs} + L_m \left(i_{dqs} + i_{dqr} \right) \tag{3}$$

Rotor flux:

$$\varphi_{dqr} = L_{ls} i_{dqr} + L_m \left(i_{dqs} + i_{dqr} \right) \tag{4}$$

Mechanical:

$$T_e = \frac{3}{2}\frac{p}{2}\left(\varphi_{ds} i_{qs} - \varphi_{qs} i_{ds}\right) \quad (5)$$

$$T_e - T_l = J_m \frac{2}{p}\frac{d\omega_r}{dt} + B_m \omega_r \quad (6)$$

Where:
$v_{dqs} = v_{ds}; v_{qs}$ = d-axis;q-axis stator voltages. $i_{dqs} = i_{ds}; i_{qs}$ = d-axis ; q-axis stator currents
$\varphi_{dqs} = \varphi_{ds}; \varphi_{qs}$ = d-axis; q-axis rotor flux linkages. $T_e; T_L$ = The electromagnetic torque; load torque

2.2. The DTC-MSVM Scheme

a) MSVM: The SVM method has been widely used in regulating PWM inverter due to a high modulation index and low harmonics of current [10]. In addition, with HP-ZSI scheme, the STS should be inserted period intervals of SVM which are called MSVM. The MSVM principle is also based on switching patterns of SVM [12]. Especially, the STS of MSVM are applied to solve problems such as boost-buck DC-link voltage of the HP-ZSI. They reduce the common voltage, not requiring dead-time protection short circuit at two switches to any of the same phase legs [3, 9].

In switching patterns of MSVM are included three zero vectors as V_0, V_7 and the third zero vector is STS. Where V_1 to V_6 are the six active vectors in Figure 1a. The V_{ref} rotates around sectors of hexagon (from 1 to 6) that V_a and V_b are edges of the hexagon, where (a,b) = (1,2); (2,3); (3,4); (4,5); (5,6) in every sector as shown in Figure 1a, respectively. Therefore, in a sampling interval V_a, V_b are combined with T_a, T_b to calculate V_{ref} as shown in (7) and Figure 1a and b, respectively. The shoot-through time (T_{sr}) are calculated as $T_{sr} = T_0 - T_0^{'}$, where $T_0^{'} = T_{sf} - \left(T_a + T_b + T_{sr}\right)$ Figure 1c). Consequently, from (7), the reference voltage vector (V_{ref}) can be given by:

$$\bar{V}_{ref} = \bar{V}_a T_a + \bar{V}_b T_b \quad (7)$$

$$T_a = \sqrt{3}.\frac{V_{ref}}{\hat{V}_i}.T_{sf}.\sin\left(\frac{\pi}{3} - \beta\right) \quad (8)$$

$$T_b = \sqrt{3}.\frac{V_{ref}}{\hat{V}_i}.T_{sf}.\sin\left(\beta\right) \quad (9)$$

Where β is the angle between the reference voltage vector V_{ref} and voltage vector V_1, $\hat{V}_i$ is the PDV.

In the MSVM, in a half switching cycle $(T_{sf}/2)$ as shown in Figure 1c), three equal-interval $(3x2T/3)$ STS will be assigned within two null intervals and within central of two active states. The STS can be assigned per switching cycle but the active interval T_a, T_b are also kept unchanged. Therefore, the STS does not affect to SVM features of the inverter and the shoot-through time (T_{sr}) is limited by $(T_{sf}/2)$ as shown in (11) and Figure 1c). In the switching cycle $\left(T_{sf}\right)$ included six equal-interval $(6x2T/3)$ STS. Hence, the shoot-through time (T_{sr}) and *T* are determined by (10).

$$T_{sr} = 6.2.\frac{T}{3} = 4.T \rightarrow T = \frac{T_{sr}}{4} \quad (10)$$

And from [32] we have:

$$o < d_0 = \frac{T_{sr}}{T_{sf}} < \frac{1}{2} \rightarrow o < T_{sr} < \frac{T_{sf}}{2} \tag{11}$$

Where d_o is shoot through duty. From (10) and (11) we have:

$$0 < T < \frac{T_{sf}}{8} \tag{12}$$

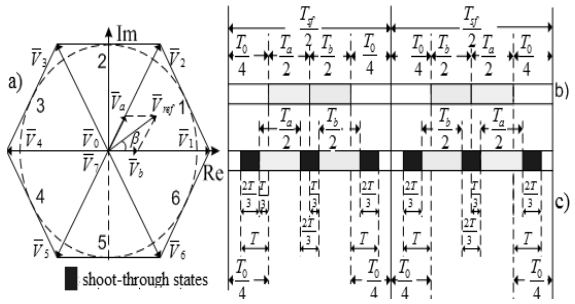

Figure 1. Traditional SVM of VSI a) Switching Patterns for Traditional SVM b) Switching Patterns of MSVM c)

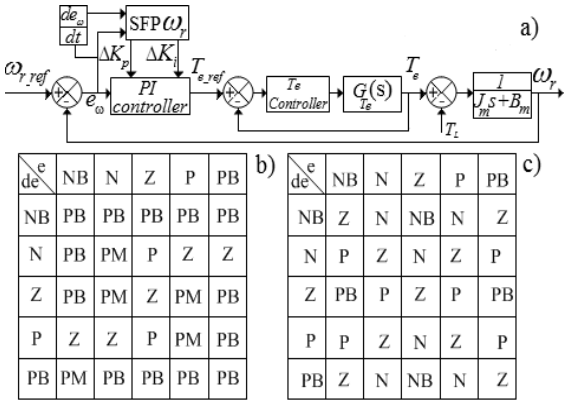

e / de	NB	N	Z	P	PB
NB	PB	PB	PB	PB	PB
N	PB	PM	P	Z	Z
Z	PB	PM	Z	PM	PB
P	Z	Z	P	PM	PB
PB	PM	PB	PB	PB	PB

e / de	NB	N	Z	P	PB
NB	Z	N	NB	N	Z
N	P	Z	N	Z	P
Z	PB	P	Z	P	PB
P	P	Z	N	Z	P
PB	Z	N	NB	N	Z

Figure 3. SFP Block Diagram a) Rules of ΔK_p b) and ΔK_i c)

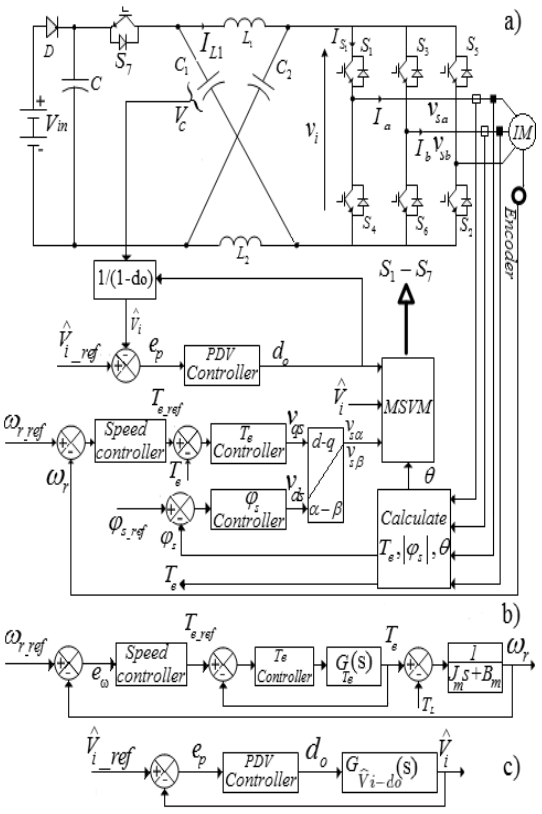

Figure 2. General DTC-MSVM Block Diagram a) SIM (ω_r) Block Diagram b) PDV ($\hat{V}_i$) Block Diagram c)

Therefore, the DCV is regulated by controlling the PDV across the inverter bridge which have to base on the limited time *T*.

b) DTC-MSVM scheme: The conventional DTC combined with the modified space vector modulation(DTC-MSVM) provided constant inverter switching frequency, achieved optimal harmonic current performance, low torque ripple compared to the traditional DTC scheme [5, 6]. The DTC-MSVM features are also the same with the DTC-SVM features such as: fast torque response, low current distortion, high performance dynamic characteristics and accuracy. Especially, the DTC-MSVM scheme as shown in Figure 2a, the value of PDV should be controlled by regulating d_0 as shown in (11) and capacitor voltage of HP-ZSI while DIV change suddenly. The PDV should be controlled well so that it does not affect to quality control of SIM, the torque of the motor and increases robustness of drive systems [5, 11, 22]. Therefore, the DTC-MSVM scheme is the best candidate for HEV applications.

2.3. Analysis of the HP-ZSI Network Modeling

To design control algorithms for controlling the PDV of HP-ZSI, we have to know a proper dynamic model of the HP-ZSI. The open-loop transfer function in s-plane $G_{\hat{V}_{i-d_o}}(s)$ of the shoot-through duty ratio (d_0) to PDV $(\hat{V}_i)$ is given in [5, 33] and Figure 2c, where the load is IM and $G_{\hat{V}_{i-d_o}}(s)$ are given in (13), Where $\hat{V}_i(s)$ is PDV in the s-plane, $d_0(s)$ is shoot through duty in s-plane. And where V_{in}; V_c; I_L; I_l; L_l; R_l ;L ;C ;D_0 are DIV, HP-ZSI capacitor voltage, steady state values of inductor current, IM current, IM inductance, IM resistance, HP-ZSI inductance, HP-ZSI capacitance, capacitor voltage and the shoot-through duty cycle at certain operating point, respectively.

$$G_{\hat{V}_{i-d_0}}(s)=\frac{\hat{V}_i(s)}{d_0(s)}=\left\{\frac{(-2I_L+I_l)L_lLs^2+\left[(-2I_L+I_l)R_lL+(1-D_0)(2V_c-V_{in})L+(1-2D_0)(2V_c-V_{in})L_l\right]s+(1-2D_0)(2V_c-V_{in})R_l}{L_lLCs^3+R_lLCs^2+\left[2L(1-2D_0)^2+L_l(1-2D_0)^2\right]s+R_l(1-2D_0)^2}\right\} \quad (13)$$

3. Intelligent Controller Design Strategies for PDV and SIM, Stator Flux and Electromagnetic Torque Controller

3.1. Speed of the Induction Motor Controllers

In closed-loop speed control of the IM is shown in Figure 2a) and b) which contain the open loop transfer function of the electromagnetic torque in s-plane as $(G_{Te}(s))$ [6, 34]. This transfer function is calculated by the electromagnetic torque $(T_e(s))$ divides the q-axis stator voltage $(V_{qs}(s))$ as shown in (14):

$$G_{Te}(s)=\frac{T_e(s)}{V_{qs}(s)}=\frac{s+A_{Te}}{s^2+B_{Te}s+C_{Te}} \quad (14)$$

$$\text{Where}: A_{Te}=\frac{K_tL_r}{\sigma};\ B_{Te}\frac{R_sL_r+R_rL_s}{\sigma};\ C_{\varphi}=\frac{3p^2K_tL_r\left|\varphi_{s-ref}\right|^2}{2J_m\sigma};\ \sigma=L_rL_s-L_m^2$$

Figure 2a and b and from (14) show that due to the influence of temperature while the DTC-MSVM operates, IM parameters are continuous variation and uncertainties or unknown parameters of this system. Therefore, adaptive intelligent control techniques such as SFP, GAs-PI will be the most suitable for features of this system.

a) Self-tuning fuzzy PI controller (SFP): When the performances of DTC-MSVM drive, its parameters are always variable on-line. If the gains of conventional PI controller are fixed, the output response will not satisfy with the varying uncertainty of IM parameters or structure is variable. Consequently, FLC is used to tune gains of the traditional PI controller on-line as shown in Figure 3a which is the most suitable for the requirements of this system.

In this control method, input signal of the FLC is the speed error (e_ω) and a derivative of the speed error (de_ω). Every input of the FLC has five triangular membership functions (TMF) with overlap and equal width. Each output of the FLC (ΔK_p, ΔK_i) has four TMF and 25 fuzzy rules which are shown in Figure 3b) and c), respectively. Moreover, these outputs are used to tune gains of the PI controller (K_p, K_i) on-line which base on a set of fuzzy rules to maintain precise speed control of the IM.

Figure 4 shows flow chart of SFP algorithm to tune gains value of the PI controller (K_p, K_i) on-line which base on [5, 6]:

If n = 0, the gain of the PI controller is taken as:

$$\begin{cases}K_p(0)=2J_m\xi\omega_n-B_m=0.47\\ K_i(0)=J_m\omega_n^2(2\xi^2-1)=1.26\end{cases} \quad (15)$$

Where J_m = 0.02($kg.m^2$), B_m = 0.005752($N.m.s$), ξ = 0.8 and ω_n = 15(rad/s) are inertia, friction factor, the desired damping and dynamic response, respectively.

Else if $n > 0$, the gains of the PI controller is calculated as:

$$\begin{cases} K_p(n) = K_p(n-1) + \Delta K_p(n) \\ K_i(n) = K_i(n-1) + \Delta K_i(n) \end{cases} \quad (16)$$

Where n is a sample time *n-th*. Thus, the speed response of the IM is improved, decrease total harmonic distortion (*THD*) of current, increase robustness of the SIM and increase performance of the drive system.

b) Genetic algorithms optimal tuning gains of the PI controller (GAs-PI): GAs is a stochastic global adaptive search optimization technique based on the mechanisms of natural selection where stronger individuals are likely the winners in a competing environment [27]. GAs has been widely recognized as an effective and efficient technique to solve optimization problems [16]. Especially, GAs is better than compared to other optimization techniques as avoiding local minima, does not require derivative information which is an ordinary aspect of nonlinear systems [17, 29]. The steps of GAs might consist of the following:

- GAs starts with an initial population containing a number of individuals (or chromosomes)
- Evaluate the fitness value for each individual in the population
- Repeat the following steps as genetic Selection, Crossover and Mutation until n offspring have been created

1. Selection: Individuals of the initial population are selected for reproduction with probability proportional to their fitness value. The purpose of the selection is to obtain a mating pool that the fittest individuals are selected according to a probabilistic rule. These individuals become a parent to be mated into the new population that is better than old population.
2. Crossover: Then the selection stage is a genetic crossover operation which is implemented between parent pairs. These parent pairs are randomly chosen from the mating pool to generate new individuals that obtain good features from their parents. The crossover operation can be a one-point or multi−point crossover and this operation is implemented with a crossover probability (p_c)

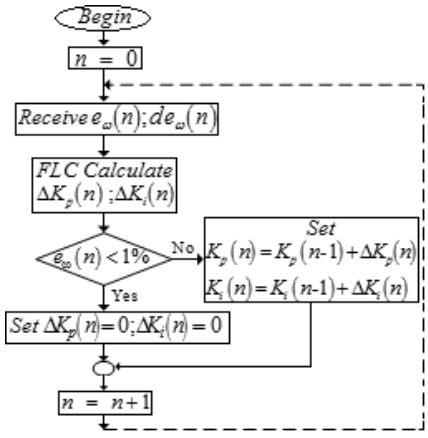

Figure 4. Flow Chart of SFP Algorithm

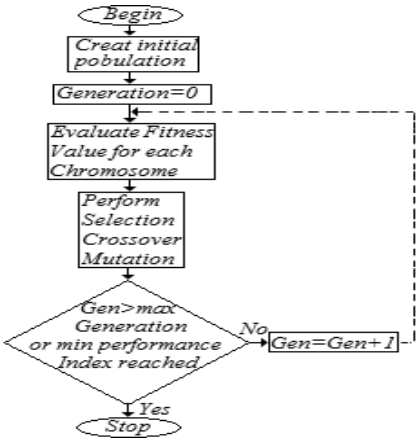

Figure 5. Flow Chart of GAs

3. Mutation: After the crossover operation is genetic mutation which performs a change in the offspring bit string to produce new individuals. These changes in the offspring bit string may represent a solution of the problem and at the same time to avoid the population falling into a local optimal point. This mutation operation is implemented with a low mutation probability (p_m) which is often to preserve good chromosomes.

- Evaluate again fitness value for each individual in the population to replace the current population into the new population.
- The algorithm stops when is satisfactory constrain conditions to reach the best individuals. Unless these conditions are satisfied, this algorithm has to return to step 2 for the next generation.

The application of these five basic steps allows the creation of new individuals that can be better than their parents. This algorithm is repeated for many generations and finally stops when is satisfactory constrain conditions to reach the best individuals which may achieve an optimum solution [16, 17, 27, 29]. Flow chart of the GAs is shown in Figure 5.

GAs effectiveness of search optimization technique of nonlinear systems, it can be applied to tune the gains of the PI controller to cope with the nonlinearities and uncertainties of parameters existing in speed control of induction motor. In this GAs, the fitness function (or cost function) is used to evaluate the individuals of each generation and this function can be chosen to be integral to the absolute value of the error (IAE) [17, 27]. The mathematical expression of this function is given as:

$$IAE = \int_0^t |e(t)| dt \tag{17}$$

GAs is used to tune gains of the PI controller which is abbreviated as GAs-PI. Furthermore, GAs is used to look for gains of the PI speed controller which minimize the cost function (IAE). Individuals make low IAE then these individuals are considered as the fittest. This cost function has the advantage of avoiding cancellation of positive and negative errors so it is used as the GAs evolution criteria. Each individual represents a solution for the PI speed controller gains and hence it consists of two genes: the first one is the K_p value and the second is the K_i value: the individual vector is [K_p K_i]. Due to the GAs is fast convergence, the range of these gains must be specified by sisotool of matlab software. The GAs parameters for the tuning of the PI speed controller gains are shown in Table 1.

c) PI speed controller: The PI controller is used to control of SIM. This PI controller is designed according to the equation (15) and [5, 6].

3.2. Peak DC-link Voltage (PDV) Controllers

a) Fuzzy logic controller (FLC): FLC has been widely used in the field of industrial control systems because it does not require a mathematical model of the control system and easy to implement. Especially, this controller can cope with variation of DIV in the DTC-MSVM drive system [17], [22], [31]. Thus, FLC will be suitable for this system.

Table 1. GAs Parameters

GAs property	Value/method
Number of generations	10
Number of chromosomes in each generation	5
Number of genes in each chromosome	2
Selection method	linear ranking selection
Crossover method	*BLX-* **α**
Crossover probability	0.9
Mutation rate	0.1

Table 4. Comparison among Control Methods

Speed control methods	SFP	GAs-PI	PI
Starting transient performance	Good	Excellent	Poor
Normal operating conditions	Very good	Good	Poor
Stator resistance variation	Very good	Good	Poor
Load torque disturbance	Excellent	Very good	Poor
Steady-state performance	Excellent	Very good	Good
Computational effort	High	High	Low

FLC has also been used to control PDV in HP-ZSI which its structure is PI type FLC as shown in [35] and the number of fuzzy sets for the PI type FLC structure has been determined experimentally using the measured PDV response.

Following to the fuzzy structure, it includes three blocks generally there are: fuzzification, fuzzy inference engine that generates the fuzzy rules, a defuzzification block. The aggregation and defuzzification are used centroid method and max-min, respectively [17, 31, 36]. The PI type FLC structure is chosen in this case which shown in Figure 6a), two inputs are the PDV error (e_p) and derivative of the PDV error (de_p). Also, one output signal of the FLC is

integrated to get the value of the the shoot-through duty ratio (d_0) as shown in Figure 6a). Each input, output of the PI type FLC has seven TMF with an overlap and equal width. Thus, the linguistic variable levels of them are assigned to seven levels such as NB= negative big; NM= negative middle; NS= negative small; Z= zero; PS= positive small; PM= positive middle; PB= positive big which is given in Figure 6b and as shown in [17, 22, 31]. Figure 6c shows fuzzy rules with 49 rules which it can be acquired from observation of reference speed tracking ability at different operating points.

The scaling factors K_1, K_2 and K_u are also determined experimentally by the observation of PDV response. These factors are used to normalize inputs (e_p, de_p) and output (d_0) are well adapted to the range [-10 10] for any operating point [17, 22, 31]. In this paper, the value of scaling factors is calculated to operate PI type FLC as K_1 = 1, K_2 = 0.0015 and K_u = 10.

b) Self-tuning fuzzy PI controller (SFP): The implementation steps of this method are also the same section 3.1.a. Due to the DIV often changes continuously over time, the best solution to this problem is to update the gains of the PI controller on-line base on a set of fuzzy rules to maintain precise of PDV in ZSI. Based on observation of reference PDV tracking ability at different operating points to design member function and fuzzy rules. Therefore, each output of the FLC (ΔK_p, ΔK_i) has four TMF and 25 fuzzy rules which are shown in Figure 7a and b. The flow chart of SFP algorithm is also shown in Figure 4.

c) PI controller: The PI controller is used to control of PDV in HP-ZSI. This PI controller is designed using the equation (13) combined with the sisotool of Matlab software [6].

3.3. Electromagnetic Torque and Stator Flux Controller

In DTC-MSVM scheme, The transfer function of electromagnetic torque and stator flux are given in [5, 6] and [37, 38] is shown in Figure 2a and b. The PI controller is also used to control electromagnetic torque and stator flux. These controllers are designed using the Equation (14) combined with the sisotool of Matlab software.

4. Simulation Results

In order to analyse comparison and evaluations for affecting of the stator resistance and load torque variation to the quality of the speed response as well as the performance of DTC-MSVM drive under the different speed control strategies as SFP, GAs-PI, PI controller. Stator resistance and load torque are chosen for this affecting because the performance of the DTC-MSVM drive is greatly affected by the variation of these parameters. Moreover, when the DIV suddenly changes, the quality of the PDV response and total harmonic distortion will greatly be affected. Hence, this paper also presents comparisons of the different techniques for controlling PDV such as FLC, SFP, PI controller. These comparisons are simulated by using Matlab software. We chose squirrel cage IM and the DTC-MSVM parameters is given in Table 2.

Figure 8a shows the electromagnetic torque (T_e) always tracks the load torque (T_L) and ripple of the electromagnetic torque is very small. Also, when the load torque is continuous variation from t=0s to t=3s, the speed response of IM under the different techniques as PI controller (blue-line), SFP (red-line) and GAs-PI (black-line) are shown in Figure 8b. The IM is started under unload operating condition at time from t = 0s to t=0.1s.

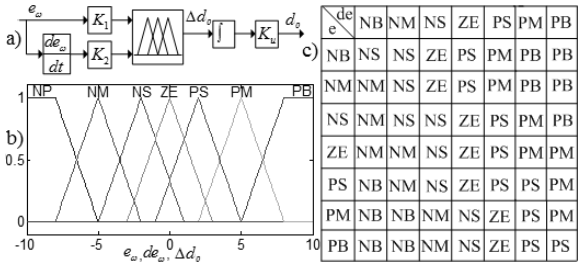

de \ e	NB	NM	NS	ZE	PS	PM	PB
NB	NS	NS	ZE	PS	PM	PB	PB
NM	NM	NS	ZE	PS	PM	PB	PB
NS	NM	NS	NS	ZE	PS	PM	PB
ZE	NM	NM	NS	ZE	PS	PM	PM
PS	NB	NM	NS	ZE	PS	PS	PM
PM	NB	NB	NM	NS	ZE	PS	PM
PB	NB	NB	NM	NS	ZE	PS	PS

Figure 6. Block Diagram of the PI-Type FLC a) Two Inputs (e_ω), (de_ω) and One Output (d_0) MF of the PI-Type FLC b) PI-Type FLC Rules c)

de \ e	NB	N	Z	P	PB
NB	–	PB	PB	PB	–
N	–	PM	P	Z	–
Z	–	PM	Z	PM	–
P	–	Z	P	PM	–
PB	–	PB	PB	PB	–

b)

de \ e	NB	N	Z	P	PB
NB	Z	N	NB	N	Z
N	P	Z	N	Z	P
Z	PB	P	Z	P	PB
P	P	Z	N	Z	P
PB	Z	N	NB	N	Z

c)

Figure 7. Fuzzy Rules of ΔK_p a) and ΔK_i b) of SFP Algorithm

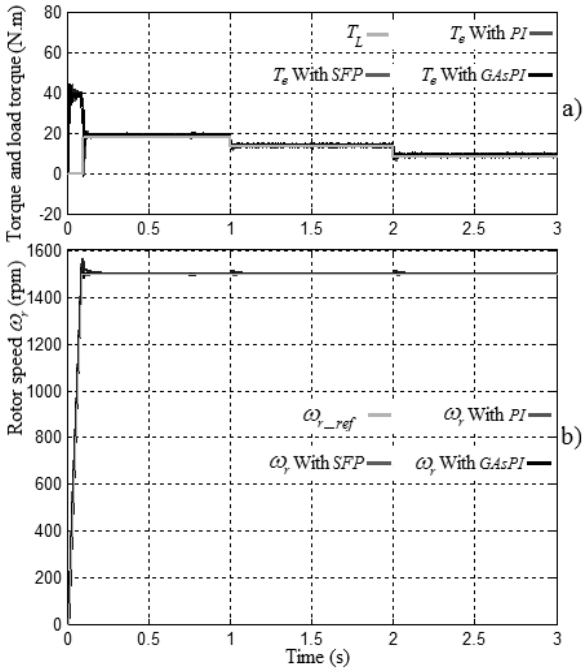

Figure 8. Electromagnetic Torque T_e and Load Torque T_L a) Speed Response using PI Controller, SFP and GAs-PI b)

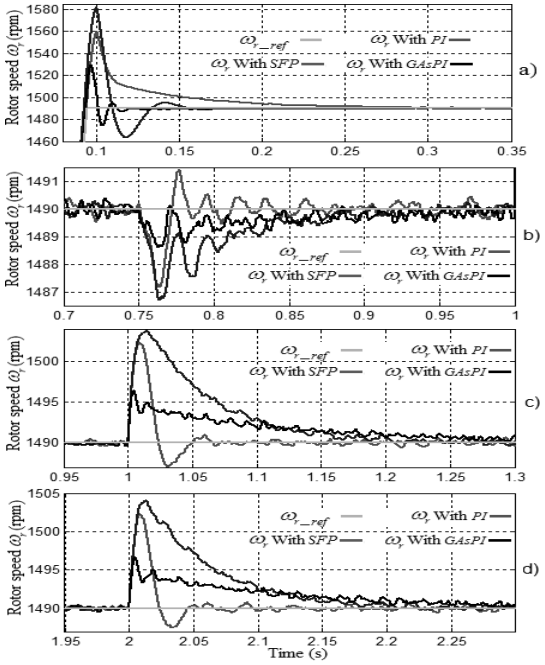

Figure 9. Starting Transient of the IM a) Speed Response During R_s Increase 50% at 0.75s b) SpeedR due to Load Change at Time 1s c) and 2s d)

The starting transient performance of the IM under three different techniques is shown in Figure 9a. The speed reference ($\omega_{r\text{-}ref}$) is 1490*rpm*, GAs-PI shows a speed overshoot of 2.6% compared to 4.7% and 6.2% of the SFP and PI controller, respectively. Moreover, the settling time with the limited of steady-state speed error percentage (e_ω% < 0.16%). The GAs-PI, SFP and PI controller show settling time as 0.12*s*, 0.23*s* and 0.15*s*, respectively. The GAs-PI shows the smallest settling time in three speed control strategies. Hence, during starting of induction motor, the GAs-PI shows the best transient response compared to SFP and PI controller.

Under normal operating conditions at the time, from t = 0.1*s* to t = 0.75*s,* the normal load torque is 18*N.m*. as given in Figure 9b which shows the speed response of the different techniques. When the stator resistance of IM suddenly changes as a step increase of 50% at t = 0.75*s*, speed responses of the GAs-PI, SFP and PI controller show speed drops to 1488.6*rmp*, 1487.2 rmp and 1486.7*rmp* then are corrected back to their demanded value (1490*rmp*) after 0.05*s*, 0.025*s* and 0.15*s*, respectively. Results show that the GAs-PI has the lowest speed drops compared to SFP and PI controller. However, the SFP shows the smallest settling time compared to GAs-PI and PI controller.

When the load torque suddenly reduces from 18N.m to 13*N.m* at *t*=1*s* as shown in Figure 8a, the speed response under the different control strategies is shown in Figure 9c. At *t*=1*s*, the GAs-PI, SFP and PI controller show speed shot to 1496.4*rmp*, 1502.2*rmp* and 1503.8*rmp* then are adjusted back to their demanded value (1490 *rmp*) after 0.2*s*, 0.05*s* and 0.21*s*, respectively, as shown in Figure 9c. Also, when the load torque suddenly reduces from 13*N.m* to 8*N.m* at *t*=2*s*, the speed response is shown in Figure 9d) which is similar to the case of the speed response at *t*=1*s*, as shown in Figure 9c. The GAs-PI shows the lowest speed shot compared to SFP and PI controller but the SFP shows the smallest settling time compared to GAs-PI and PI controller. Therefore, in order to evaluate which control methods are the most suitable for the DTC-MSVM scheme, we have to calculate cost function (IAE) as shown in (17). This calculation is based on the speed error of the IM.

The DIV can battery or fuel cell which is used to make voltage source to supply the DTC-MSVM drive system. Consequently, the purpose of improving the response of PDV is to increase output voltage stabilization in HP-ZSI, decrease phase current harmonic spectrum in

order to improve the performance of the DTC-MSVM drive system [11], [22]. Figure 10a) shows characteristic assumed of the DIV. Also, Figure 10b) shows the PDV response under the different techniques. Where the value of PDV reference $(\hat{V}_{i-ref})$ is chosen as 560*V*, the FLC (black-line), SFP (red-line) and PI controller (blue-line) are shown in Figure 10b) and transient response of PDV under these control methods is similar.

Table 2. Parameters Used for Simulation of DTC-MSVM

Parameter	Value
Z-source inductance (L_1 and L_2) (mH)	0.4
Z-source capacitance (C_1 and C_2) (mF)	0.5
Nominal power (P_n) (W), voltage (V_n) (V)	3760; 400
Frequency (f_n) (Hz)	50
Stator resistance (R_s) (Ω)	1.115; 1.6 at t=0.75s
Rotor resistance (R_r) (Ω)	1.083
Stator (L_s); rotor (L_r) inductance (H)	0.006;0.006
Magnetizing inductance (Lm) (H)	0.2037
Switching frequency (f_{sf}) (kHz)	10
Pole pairs (p)	2
Inertia (J_m) ($kg.m^2$)	$2*10^{-2}$
Friction factor (B_m) (N.m.s)	$5.752*10^{-3}$
DC-link peak voltage($\hat{V}_{i-ref}$)(V)	560
DC input voltage (V_{in}) (V)	500, t=0s; 450, t=1s; 400, t=2s
Speed motor (ω_{r-ref}) (rpm)	1490
load torque (T_L) (N.m)	18, t=0.1s; 13, t=1s; 8, t=2s

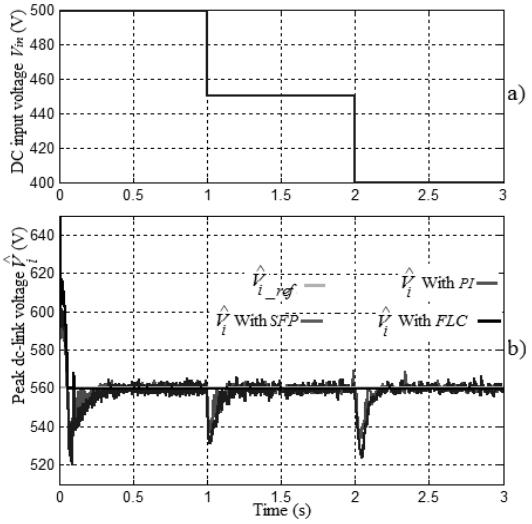

Figure 10. DIV Decrease 10% at 1s and Continue Decrease 10% at 2s a) PDV Response Due to DIV Change b)

When the DIV suddenly reduces from 500*V* to 450*V* at *t*=1*s*, the FLC shows the PDV response tracks the PDV reference with good but the SFP and PI controller show PDV drops to 538V and 530V then are adjusted back to their demanded value (560V) after 0.15s, 0.25s, respectively, as shown in Figure 10b. Moreover, when the DIV suddenly reduces from 450*V* to 400*V* at *t*=2*s* as shown in Figure 10a, the FLC also shows the PDV response always tracks the PDV reference. However, the SFP and PI controller show PDV drops to 536*V* and 522*V* then are adjusted back to their demanded value (560V) after 0.17*s*, 0.27*s*, respectively, as shown in Figure 10b. Results from Figure 10b show that the PDV is controlled by FLC which is the most robust against variation of DIV compared to the SFP and PI controller.

Figure 11 shows total harmonic distortion of current (*THD*%) under the different control strategies. From analysis as shown Figure 9, the SFP and GAs-PI is used to control the SIM which are better than PI controller. Assume that the SIM is controlled by the GAs-PI, in order to give a comparison of total harmonic distortion of current (*THD*%) under three control techniques for the PDV such as PI controller, SFP and FLC. If the PI controller is used to control the PDV and the GAs-PI is used for controlling the SIM, the combined of the two strategies is abbreviated as PI-GAsPI which has (blue-line) as shown in Figure 11. Similar as analysis above, there are SFP-GAsPI (red-line) and FLC-GAsPI (black-line) which are shown as in Figure 11. Results from Figure 11 shows that the FLC-GAsPI has the lowest *THD*% = 3.38% compared to the SFP-GAsPI *THD*% = 3.64% and PI-GAsPI *THD*% = 4.57%. Therefore, FLC is the most suitable for controlling PDV in HP-ZSI of DTC-MSVM scheme.

In order to give a clear concept of the performance index of the different control strategies, the IAE is used to calculate for each technique during three stages as normal operating conditions, load torque variation and stator resistance variation. During these stages, FLC is chosen to control PDV. Moreover, the SIM is controlled by GAs-PI (black-line), SFP (red-line), PI controller (blue-line) as shown in Figure 12 a, b, c, d and e.

During normal operating conditions, from *t*=0*s* to *t*=0.75*s*, GAs-PI shows the lowest IAE value compared to SFP and PI controller. During stator resistance variation, from *t*=0.75*s* to *t*=1*s* and normal load torque is 18N.m, SFP shows the lowest IAE value compared to GAs-PI and PI controller as shown in Figure 12b. When the load torque suddenly changes from 18*N.m*

to 13*N.m* takes place at *t*=1*s* and the load torque suddenly also reduces from 13*N.m* to *8N.m* at *t*=2*s*, SFP also shows the lowest IAE value compared to GAs-PI and PI controller, as shown in

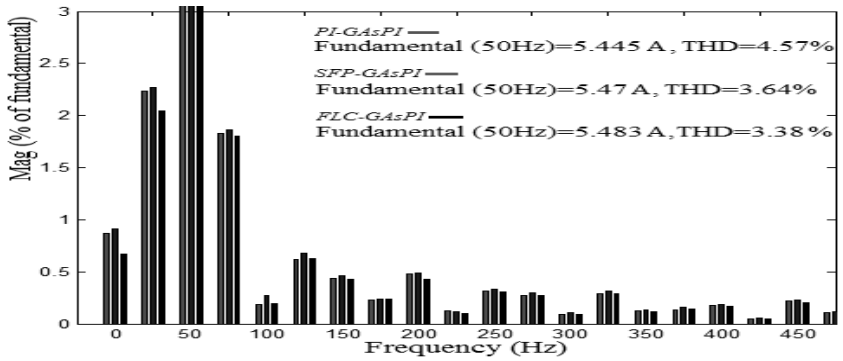

Figure 11. THD% using PI controller for PDV and GasPI controller for speed IM (PI-GAsPI), SFP-GAsPI and FLC-GAsPI

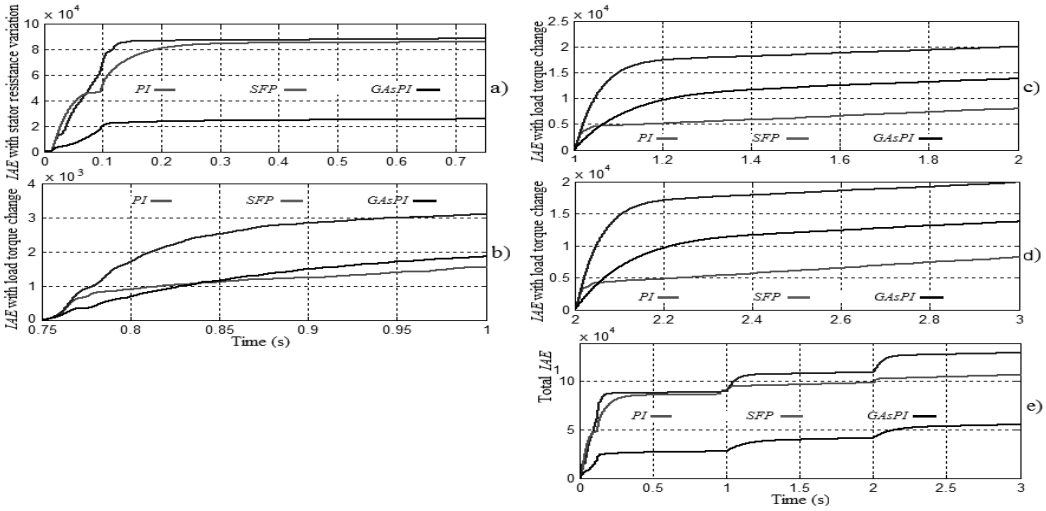

Figure 12. IAE with Normal Operating Conditions a) IAE with Stator Resistance Variation at 0.75s b) IAE with Load Torque Changes at 1s c) IAE with Load Torque Changes at 2s d) Total IAE e)

Figure 12c and d. However, during simulation process, from *t*=0*s* to *t*=3*s*, the GAs-PI shows the lowest total IAE value compared to SFP and PI controller, as shown in Figure 12e. A comparison between the three controllers is given in Table 3.

Table 3. Summary of Results of the Different Speed Control Strategies

The different speed control strategies	SFP	GAs-PI	PI controller
IAE(t[0s,0.75s])	85654	25484	88200
IAE(t[0.75s,1s])	1539.3	1862.6	3094.4
IAE(t[1s,2s])	7984.2	13795	20014
IAE(t[2s,3s])	8249.5	13749	19915
Total IAE(t[0s,3s])	103427	54891	131223.4
Speed overshoot(%), settling time (s) (limited of the steady-state speed error *e!*% < 0:16%)	4.7%, 0.23s	2.6%, 0.12s	6.2%, 0.15s
Stator resistance suddenly increases a 50% at t = 0.75s, speed drop(rmp), settling time(s)	1487.2, 0.025s	1488.6, 0.05s	1486.7, 0.15s
Load torque suddenly changes from 18N.m to 13N.m at t=1s, speed shoot(rmp), settling time(s)	1502.2, 0.05s	1496.4, 0.2s	1503.8, 0.21s
Load torque suddenly changes from 13N.m to 8N.m at t=2s, speed shoot(rmp), settling time(s)	1502.2, 0.04s	1496.4, 0.2s	1503.8, 0.2s

5. Discussion

The FLC has been used to control the PDV, the actual value of PDV tracks the reference value of PDV with good and this controller also shows the lowest *THD*% compared to the SFP and PI controller. Compared to the SFP and PI controller, FLC shows the most robust against variation of the DIV.

The SIM is controlled by the different control strategies as GAs-PI, SFP, PI controller. Simulation results show that under normal operating conditions, using GAs-PI to control the speed is very good, giving small drift, and shows the lowest IAE value compared to SFP and PI controller. However, when the load torque and stator resistance suddenly change, GAs-PI shows a low torque disturbance rejection capability and shows a low robustness against stator resistance variation due to the fixed gains controller.

Generally, the GAs-PI is algorithm tuning gains of the PI controller off-line. This algorithm may need a lot of convergence time to achieve an optimum solution, depending on the choice of the parameters of GAs-PI and the complexity of the drive system. In order to decrease the convergence time, the parameters of GAs-PI such as the range of the PI controller gains must be determined and limited before. Moreover, the number of generations, the number of chromosomes in each generation must be selected appropriately to ensure the convergence capability of the algorithm. Furthermore, GAs-PI can be used to tune the PI controller gains on-line, however the updating time will be short depending on the rate of microcontroller and the convergence rate of the algorithm.

The self-tuning capability of the SFP is on-line, SFP is used for controlling the SIM to cope variation of IM parameters. This algorithm is implemented to base on the speed error and derivative of the speed error in order to tune the gains of the PI controller on-line by using fuzzy rules. During stator resistance variation and a load torque disturbance, SFP shows the lowest IAE value compared to GAs-PI and PI controller. SFP also shows that the actual SIM tracks the reference speed with good. In this condition, the GAs-PI is not tuned to the PI controller gains on-line to cope with variation of the above parameters, GAs-PI shows speed response to be not as good as the SFP. Due to the characteristics of the drive system are stator resistance variation and a load torque disturbance and If DTC-MSVM system operates in a long time, SFP looks promising and has the best robust against parameters variation of the IM and the lowest steady state performance compared to GAs-PI and PI controller.

GAs is used to look for gains value of the PI speed controller which minimize the cost function (IAE) before the DTC-MSVM drive system operates. Consequently, during the starting of the IM that the parameters of its have not changed yet, the GAs-PI shows the best transient response comparison to SFP and PI controller. Hence, the GAs-PI shows the lowest IAE value compared to SFP and PI controller under motor starting conditions. Furthermore, during the simulation process (from $t = 0s$ to $t = 3s$), this algorithm shows the lowest total IAE value compared to SFP and PI controller. Due to the value of IAE when using GAs-PI is very small under motor starting conditions and thus this result greatly affects the total IAE value. When the DTC-MSVM system operates in a long time, GAs-PI can not be suitable for controlling of the SIM. Therefore, the SFP is still suitable for controlling the SIM in the DTC-MSVM system. Comparison among controllers is given in Table 4.

6. Conclusion

This paper presents a comprehensive analysis comparison and evaluations of the different control strategies such as PI controller, SFP and GAs-PI for controlling the SIM as well as using PI controller, FLC and SFP to control the PDV. Excepted to the PI controller, these control strategies are based on artificial intelligence techniques that do not need determined mathematical modelling of the drive system.

Results show that, under normal operating conditions or under starting conditions of the IM, GAs-PI shows the best transient response of the SIM compared to SFP and PI controller. However, the GAs-PI needs modifications to adapt on-line for the stator resistance variation and a load torque disturbance. In this condition, SFP looks promising and this algorithm shows more robust against the stator resistance variation and a good disturbance rejection capability compared to the GAs-PI and PI controller. Moreover, the SFP still needs some modifications to increase the quality of transient response of the SIM.

With the PDV in HP-ZSI, the FLC has been applied to control the PDV, giving smallest drift and the lowest *THD*% compared to the SFP and PI controller. Therefore, FLC is the most suitable for controlling the PDV in HP-ZSI.

References

[1] M Olzwesky. *Z-source inverter for fuel cell vehicles.* US Department of Energy, Freedom CAR and Vehicles Technologies, EE-2G 1000 Independence Avenue. Washington. D.C. 2005; 20585-0121,

[2] K Holland, M Shen, FZ Peng. *Z-source inverter control for traction drive of fuel cell-battery hybrid vehicles*. Industry Applications Conference Fourtieth IAS Annual Meeting. 2005; 3(4): 1651–1656.

[3] I Poh Chiang Loh, Member, DM Vilathgamuwa I, Senior Member, YS Lai, GT Chua, I Yunwei Li, Student Member. *Pulsewidth modulation of z-source inverters*. IEEE Transactions on Power Electronics. 2005; 20(6): 1346–1355.

[4] X Ding, Z Qian, Shuitao, YB Cui, F Peng. *A high-performance z-source inverter operating with small inductor at wide-range load*. Applied Power Electronics Conference, APEC, Twenty Second Annual IEEE. 2007: 615–620.

[5] O Ellabban, JV Mierlo, P Lataire. *Direct torque controlled space vector modulated induction motor fed by a z-source inverter for electric vehicles*. Proceeding International Conference on Power Engineering, Energy and Electrical Drivers, Malaga, Spain. 2011.

[6] AW Shen, CT Pham, PQ Dzung, NB Anh, LH Viet. *Using fuzzy logic self-tuning pi controller in z-source inverter for hybrid electric vehicles*. World Conference on Science and Engineering, Hong Kong, China. 2012.

[7] A Haddoun, M Benbouzid, D Diallo, R Abdessemed, J Ghouili, K Srairi. *Comparative analysis of control techniques for efficiency improvement in electric vehicles*. Vehicle Power and Propulsion Conference, VPPC. 2007: 629–634.

[8] M Vasudevan, R Arumugam. *New direct torque control scheme of induction motor for electric vehicles*. 5th Asian Control Conference. 2004: 1377–1384.

[9] AW Shen, CT Pham, PQ Dzung, NB Anh, NX Phu. A comparison of control methods for z-source inverter. *Journal of Energy and Power Engineering*. 2012; 04(04): 187–195.

[10] T Chun, Q Tran, J Ahn, J Lai. *AC output voltage control with minimization of voltage stress across devices in the z-source inverter using modified SVPWM*. PESC 37th IEEE. 2006: 1–5.

[11] X Ding, S Yang, Z Qian, B Cui, F Peng. *A direct peak dc-link boost voltage control strategy in z-source inverter*. Applied Power Electronics Conference, APEC, Twenty Second Annual IEEE. 2007; 648–653.

[12] Q Tran, I Tae, Won Chun, Member, J Ahn, I Hong, Hee Lee, Member. Algorithms for controlling both the dc boost and ac output voltage of z-source inverter. IEEE Trans. Industrial *Electronics*. 2007; 54(5): 2745–2750.

[13] D Khaburi, H Rostami. Controlling the both dc boost and ac output voltages of a z-source inverter using neural network controller with minimization of voltage stress across devices. *Iranian Journal of Electrical and Electronic Engineering*. 2011; 07(01): 60–69.

[14] KAO Om, TA agglund. *The future of PID control.* Control Engineering Practice 9, Lund, Swedena. 2001: 1163-1175.

[15] H Ur Rehman, R Dhaouadi. A fuzzy learning sliding mode controller for direct eld-oriented induction machines. *Journal of Neurocomputing*, pp. 2693–2701, May 2008.

[16] SM Gadoue, D Giaouris, JW Finch. *Genetic algorithm optimized PI and fuzzy sliding mode speed control for DTC drives*. Proceedings of the World Congress on Engineering. 2007; I.

[17] SM Gadoue, D Giaouris, JW Finch. Articial intelligence-based speed control of dtc induction motor drivesa comparative study. *Electric Power Systems Research.* 2009*;* 79(01): 210–219.

[18] S Belkacem, F Naceri, R Abdessemed. A novel robust adaptive control algorithm and application to DTC-SVM of ac drives. *Serbian Journal Of Electrical Engineering*. 2010; 07(01): 21–40.

[19] M Messaoudi, H Kraiem, MB Hamed, L Sbita, MN Abdelkrim. A robust sensorless direct torque control of induction motor based on mras and extended kalman filter. *Leonardo Journal of Sciences*. 2008; 12(01): 35–56.

[20] FJ Lin, HJ Shieh, KK Shyu, PK Huang. On-line gain tuning IP controller using real-coded genetic algorithm. *Electric Power Systems Research.* 2004; 72: 157-169.

[21] H Zhang, D Liu. *Fuzzy Modeling and Fuzzy Control*. NEW YORK, USA: Birkhauser, 2006.

[22] X Ding, Z Qian, S Yang, B Cui, F Peng. *A direct dc-link boost voltage pid-like fuzzy control strategy in z-source inverter*. Power Electronics Specialists Conference, PESC IEEE. 2008: 405–411.

[23] HWMN Uddin. *Development of a self tuned neuro-fuzzy controller for induction motor drives*. Proceedings of the Industry Applications Conference, 39th IAS annual meeting. 2004: 2630-2636.

[24] D Vukadinovic, M Basic, L Kulisic. Stator resistance identification based on neural and fuzzy logic principles in an induction motor drive. *Neurocomputing.* 2010; 73(4-6): 602612.

[25] RAL Mokrani. *A fuzzy self-tuning PI controller for speed control of induction motor drive*. Piscataway, NJ, USA. 2003; 785-790.

[26] MKA Hazzab, IK Bousserhane. Design of fuzzy sliding mode controller by genetic algorithms for induction machine speed control. *Int. Journal Emerging Electric Power Syst*. 2004; 1: 1016-1027.
[27] P Castillo. *Type-2 Fuzzy Logic in Intelligent Control Applications*, prof.janusz kacprzyk ed. Tijuana Institute of Technology, Mexico, Springer. 2011.
[28] A Rubaai, P Young, A Ofoli, T Marcel J, Castro Sitiriche. *Power Electronics Handbook (Third Edition),* Washington, DC 20059, USA , Elsevier. 2011
[29] M Chebre, A Meroufel, Y Bendaha1. Speed control of induction motor using genetic algorithm-based pi controller. *Journal of Acta Polytechnica Hungarica*. 8(6).
[30] ATEGLFF Barrero, A Gonzalez. Speed control of induction motors using a novel fuzzy sliding mode structure. *IEEE Trans. Fuzzy Syst.,* 2002; 10: 375-383.
[31] BK bose. *Modern power Electronics and AC Drivers*. USA: Pearson Education 2002.
[32] I Fang Zheng Peng, Senior Member. Z-source inverter. *IEEE Trans.Industry Applications.* 2003; 39(2): 990–997.
[33] I Poh Chiang Loh, Member, DM Vilathgamuwa, I Senior Member, YS Lai, GT Chua, I Yunwei Li, Student Member. Transient modeling and analysis of pulse-width modulated z-source inverter. *IEEE Transactions on Power Electronics*. 22(2).
[34] A Khedher, MF Mimouni. *Sensorless-adaptive dtc of double star induction motor"* Energy Conversion and Management51. 2010; 51(12): 2878–2892.
[35] P Escamilla-Ambrosio. *A novel design and tuning procedure for PID type fuzzy logic controllers*" in Intelligent Systems. Proceedings First International IEEE Symposium. 2002: 36–41.
[36] Zulfatman, MF Rahmat. Application of self-tuning fuzzy PID controller on industrial hydraulic actuator using system identification approach. *International Journal on Smart Sensing and Intelligent Systems.* 2009; 02(02): 246–261.
[37] J Li, R Qu, Y Chen. Construction Equipment Control Research Based on Predictive Technology. *TELKOMNIKA Indonesian Journal of Electrical Engineering.* 2012; 10(5): 960-967.
[38] W Jiuhe, W Mian, Z Li, Y. Hongren. Research on Passivity based Controller of Three Phase Voltage Source PWM Rectifier. *TELKOMNIKA Indonesian Journal of Electrical Engineering*. 2012; 10(5): 940-946.